An analysis of carrier dynamics in methylammonium lead triiodide perovskite solar cells using cross-correlation noise spectroscopy

Kevin Davenport[1*], Fei Zhang[2], Mark Hayward[1], Logan Draper[1], Kai Zhu[2], Andrey Rogachev[1]

[1]Department of Physics and Astronomy, University of Utah, Salt Lake City, UT, 84112, USA.,
[2]National Renewable Energy Laboratory, Golden, CO, 80401, USA.

[*]Corresponding Author: kevin.davenport@utah.edu

Abstract

Using cross-correlation current noise spectroscopy, we have investigated carrier dynamics in methylammonium lead triiodide solar cells. This method provides a space selectivity for devices with planar multi-layered structure, effectively amplifying current noise contributions coming from the most resistive element of the stack. In the studied solar cells, we observe near full-scale shot noise, indicating the dominance of noise generation by a single source, likely the interface between the perovskite and the spiro-OMeTAD hole-transport layer. We argue that the strong $1/f$ noise term has contributions both from the perovskite layer and interfaces. It displays non-ideal dependence on photocurrent, $S \propto I^{1.4}$ (instead of usual $S \propto I^2$), which is likely due to current-induced halide migration. Finally, we observe generation-recombination noise. We argue that this contribution is due to bimolecular recombination in the perovskite bulk absorption layer. Extrapolating our results, we estimate that at the standard 1 sun illumination the electron-hole recombination time is 5 microseconds.

To meet ever-increasing energy needs, a great deal of research has gone into finding cheap alternatives to silicon photovoltaics. One of the most promising materials are hybrid organic-inorganic perovskite solar cells (PSCs), which by now have reached certified power conversion efficiencies of more than 25% [1,2,3,4]. These materials have the chemical formula ABX_3, where A represents an organic cation, typically methylammonium ($CH_3NH_3^+$ or MA^+), B is a metal such as Pb^{2+} or Sn^{2+}, and X is a halide anion such as Cl^-, Br^-, or I^-. These perovskites have low processing costs [3] coupled with attractive qualities such as high carrier mobilities, long lifetimes and diffusion lengths [5], shallow intrinsic defect states [6], and low exciton binding energies [7]. The canonical perovskite, and the one studied in this work, is methylammonium lead triiodide, $MAPbI_3$.

While much attention has been given to understanding the physics of the perovskite absorber layer, less is known about the carrier dynamics at the interfaces between this layer and the electron and hole transport layers (ETL and HTL, respectively). One of the most commonly used HTL materials is the organic 2,2',7,7'-tetrakis(N,N-di-*p*-methoxyphenyl-amine)9,9'-spirobifluorene (spiro-OMeTAD). Despite its popularity, there is still a limited understanding of its hole-transport properties. Spiro-OMeTAD films tend to be amorphous, requiring doping [8] and making device reproducibility difficult. The material also suffers photoinduced alterations [9]. Similarly, the typical TiO_2 ETL can introduce hysteresis and charge-trapping effects [10] and must be annealed at high temperature.

Here, we use cross-correlated current noise spectroscopy to characterize relaxation processes in hybrid perovskite solar cells. We argue that this method has a certain *spatial* selectivity which magnifies contributions from the most resistive elements of the stack. In the perovskites, this is the ETL/perovskite/HTL interfaces.

Noise spectroscopy analyzes fluctuations of a signal from its steady-state value. It has been used to characterize defects in semiconducting devices [11,12,13], crystalline solar cells [14], light-induced defects in *a*-Si:H [15] as well as carrier kinetics [16] and metastable states [17] in perovskite solar cells. The technical advantage of our work comes from the cross-correlation technique [18], which provides several orders of magnitude better sensitivity and bandwidth than standard noise measurements. Using this technique, we have resolved the shot noise contribution in fluorescent [19] and phosphoresecent [20] organic light emitting diodes (OLED).

Figure. 1(a), shows the stack structure and energy diagram [21] of the devices studied, referenced to a zero vacuum level. They consist of a 60-nm-thick compact TiO_2 layer grown on a fluorine-doped tin oxide (FTO)/glass substrate. The $MAPbI_3$ absorption layer was spin coated at two different thicknesses, d = 200 nm

(device S7) and 800 nm (device S12) followed by a spin-coated 180-200-nm-thick spiro-OMeTAD layer topped with gold contacts. The active area of the device is 18 mm^2.

Each cell was illuminated through the substrate using an LED with a peak wavelength of 585-595nm. The devices' $I(V)$ characteristics displayed a hysteresis, as shown in Fig. 1(b). Previous studies suggest that this due to halide ion migration through the perovskite structure [22]. To avoid drift in the data, the noise spectra were taken under short-circuit conditions and after "light-soaking" illumination for 30 minutes for each light intensity.

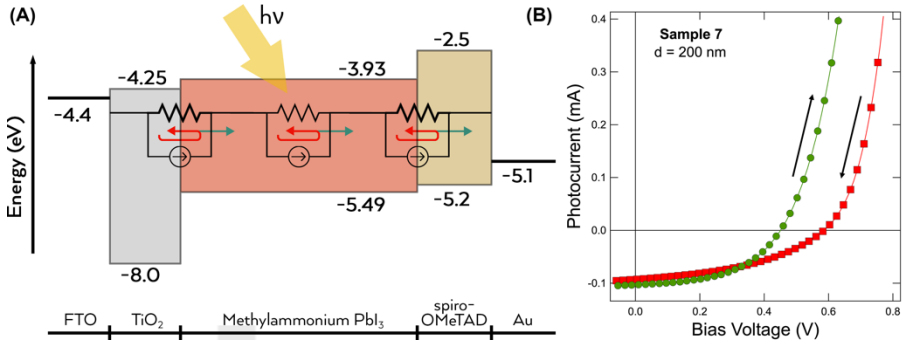

Fig. 1. (a) Device energy diagram; overlaid is noise circuit representing interfacial and bulk shot noise sources. (b) A typical $I(V)$ curve illustrating the observed device hysteresis.

Figure 2(a) shows noise spectral density curves for device S12 ($MAPbI_3$ thickness 800 nm) under different illuminations. The legend shows the corresponding short-circuit current, I_{SC} and the black curves represent a chi-squared minimization fit to the equation

$$S_I = S_1 + \frac{S_2}{f^a} + \mathrm{Re}\left[\frac{S_3}{1+(i2\pi f\tau)^{1-b}}\right] + Kf^2. \qquad (1)$$

This equation represents the fact that the observed noise spectra are the incoherent sum of the spectra from individual mechanisms. The first term is a frequency-independent term which includes thermal noise, the second represents $1/f$ flicker noise, and the third is a generalized generation-recombination (GR) noise allowing for the non-Lorentzian dispersion of the relaxation time τ. This dispersion signifies processes with a range of time scales, such as trapping/release from defect states with a range of energy levels. Note that when $b = 0$, the GR term reverts to the familiar Lorentzian profile. The final term, Kf^2, describes the residual noise background increase caused by device capacitance as discussed in details in our previous works [19, 20].

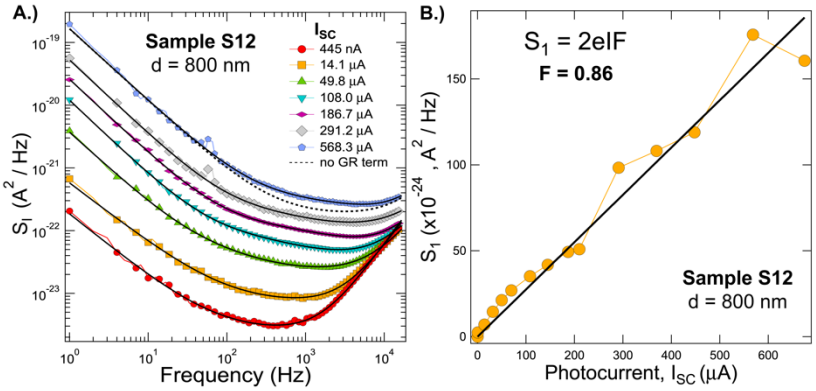

Fig. 2. Current noise data for S12 sample (a) Current noise spectral density versus frequency. Solid lines are fits to the Eq. 1. The dashed black line shows a fit to Eq. 1 where $S_3 = 0$, illustrating the existence of GR noise. (b) Frequency-independent noise term S_1 versus photocurrent; a linear fit, shown as a solid black line, gives Fano factor $F = 0.86$.

During the fitting procedure, the lowest illumination spectrum was fit first and the values of the exponents a and b, as well as the capacitive upturn term, were extracted and fixed for the rest of the spectra. Importantly, it was seen that the GR term was necessary for fit convergence. The dashed line seen in Fig. 2(a) represents a fit to Eq. 1 which uses identical fitting procedures as the solid lines except for the exclusion of the GR term, highlighting the importance of this term to reach an accurate fit.

A plot of the frequency-independent term, S_1, versus photocurrent is shown in Fig. 2(b). The linear trend indicates shot noise; fit to the dependence $S_1 = 2eFI$ returns Fano factor $F = 0.86$.

The noise spectra for the thinner S7 solar cell are shown in Fig. 3a. Compared to the thicker S12 solar cell, no GR feature is resolved. The simplest explanation is that GR term is also present in S7 and, while unresolved on its own, provides a boost to the Fano factor, shifting it to a super-Poissonian ($F > 1.1$) value (Fig. 3b).

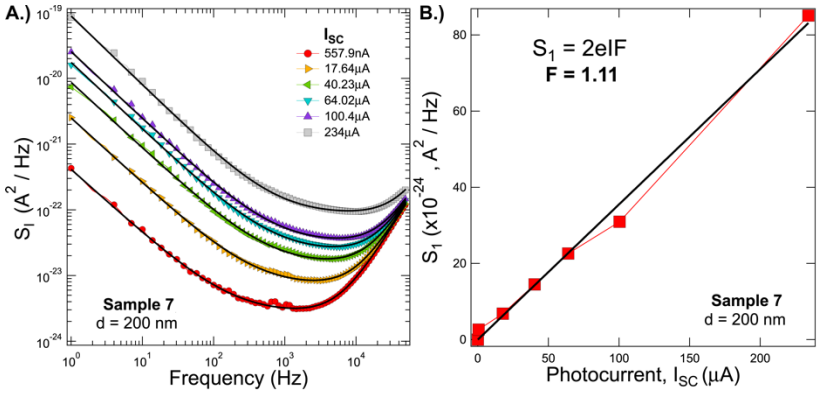

Fig. 3. Current noise data for sample S7 ($MAPbI_3$ thickness d = 200 nm) (a) Noise spectral density versus frequency for indicated photocurrents. The black curves are fits to Eq.1 with GR magnitude set to zero (b) Frequency-independent noise extracted from the fits in (a) yielding a Fano factor of F=1.1.

The appearance of $F < 1$ in the thick device is more interesting. To first approximation, the total shot noise can be represented by a series of noise sources, i_n, each self-shorted by its own internal resistance, R_n as shown in Fig. 1a. From Kirchhoff's law, the total noise current seen at the contacts is $I_T = \sum_n (i_n R_n) / R_T$, where R_T is the total device resistance. Assuming that all noise generators are uncorrelated shot noise sources, the total current noise seen at the electrodes is

$$\left\langle I_T^2 \right\rangle = \sum_n \left\langle i_n^2 \right\rangle \left(\frac{R_n}{R_T} \right)^2 = 2eI \sum_n \left(\frac{R_n}{R_T} \right)^2 = 2eIF \,. \qquad (2)$$

The sum in Eq. 3 is dominated by the most resistive term and this feature adds an important *spatial selectivity* to the noise signals. This approach is a general one describing a standard procedure for analyzing the noise contributions of lumped elements and has been used, for instance, to analyze noise generated by hopping transport in both organic [19, 20] and inorganic [23] devices. It is important to note that this procedure can be used to describe *any* noise source, though the extension is not as straight-forward as 1/*f* and GR noise lack a fundamental mechanism fixing the magnitude and frequency range. Within the the lumped-element model we use, this means that each interface and bulk section of the stack is represented by several noise sources connected in parallel to each other and to a resistor of this section. However, due to fact that specific mircoscopic processes dominate only in specific ranges of the frequency spectrum, accounting for all possible terms is rarely needed. For simplicity, only an single noise source is shown in Fig.1(a).

Shot noise reflects the discreet nature of electric charge and appears due to the random transfer of charge carriers across an energy barrier. In our experiment, the close-to-unity value of the Fano factor indicates the dominant contribution of a single resistive element in the stack. Given the abrupt interface between the perovskite and the spiro-OMeTAD HTL, it is likely that the shot noise is dominated by a Schottky barrier at this interface. That this is interfacial is further indicated by the observation that the Fano factor remains relatively constant even as the thickness of the $MAPbI_3$ layer is greatly increased. Indeed, if the bulk were a significant source of shot

noise, the Fano factor would actually decrease according to Eq. 2, assuming the interfaces remain the same across devices.

Figure. 4a shows the 1/*f* noise magnitude in log-log scale, S7 device in red (circles) and S12 in yellow (squares). The magnitude of the noise in S7 is roughly twice as large than in S12. Assuming that the interfacial properties in both devices are the same, the larger noise in S7 should come from the enhanced 1/*f* noise in the bulk perovskite layer. This is an expected tendency. Indeed, in inorganic semiconductors, enhanced 1/*f* noise is predicted to follow the dependence $\left\langle S_{1/f} \right\rangle \propto I^2 / \Omega$ [24], where Ω is the sample volume, a trend which holds for either mobility or concentration fluctuations [24]. In the analysis of 1/*f* noise, we again use the reasoning based on Eq. 2. The very fact that we observe dependence of noise on perovskite thickness suggests the 1/*f* noise generator for bulk perovskite layer has much larger magnitude than 1/*f* noise coming from interfaces.

We further notice that the 1/*f* noise dependence on current is $S_{1/f} = AI^{\alpha}$ with an exponent $\alpha \approx 1.5$. Deviation from the standard value $\alpha = 2$ suggests the presence of traps induced by current or light [25]. Our results suggest that the induced defects are present both in the bulk perovskite layer and at interfaces. The likely source of these current-driven defects is the often observed migration and interfacial collection of the halide ions [26], though its exact origin cannot be established solely from noise measurements.

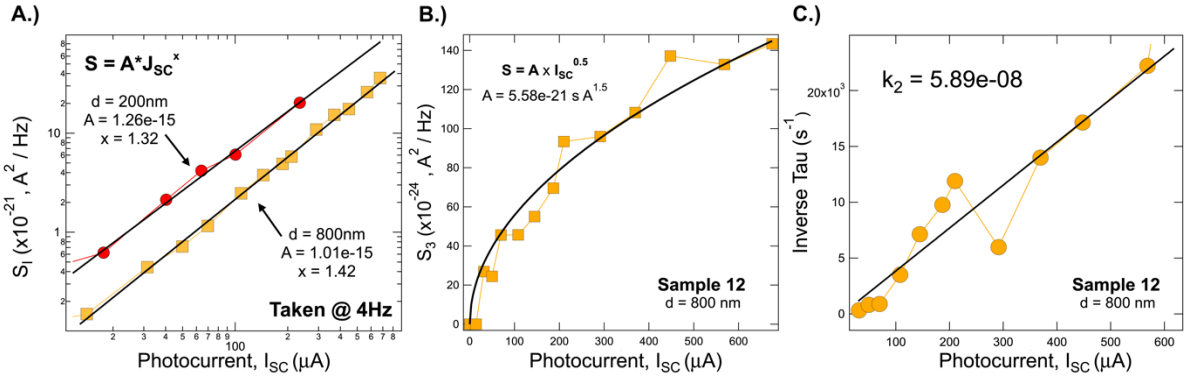

Fig. 4. (a) Log-log flicker noise, sampled at 4 Hz, in the S7 and S12 devices as a function of photocurrent. Black lines represent a fit to a generic power law. (b) The GR noise magnitude as a function of photocurrent, showing a square root dependence. (c) Extracted GR timescale as a function of photocurrent.

Figure 4(b) shows the magnitude of the GR noise as a function of photocurrent, which appears to follow a square-root dependence. The relaxation exponent, *b*, was found to be 0.32, indicating a moderate dispersion of the relaxation time. Most importantly, the inverse relaxation time was found to vary linearly with photocurrent (Fig 4(c)).

Phenomenologically, the recombination rate in semiconductors depends on the number of carriers involved in the elementary recombination process and, in the simplest case when electrons and holes have the same concentration n, can be written as [27,28], $R(n) = k_1 n + k_2 n^2 + k_3 n^3$. The three terms in this equation represent monomolecular recombination involving an intermediate step of capture by a trap, bimolecular recombination involving two carriers as in band-to-band recombination, and trimolecular recombination involving a third particle as in an Auger process. Noise spectroscopy measures relaxation time of small fluctuations from a steady state value n_0, which is $\tau = \left(\partial R(n) / \partial n\right)^{-1}_{n_0}$. Under constant illumination, the solar cell photocurrent is proportional to the steady state, non-equilibrium concentration of carriers. Hence, the experimentally observed linear dependence of $1/\tau$ on current allows us identify the microscopic process as bimolecular recombination, $1/\tau = 2k_2 n_0 \propto I_{SC}$.

To compare our results quantitatively with values of the recombination time obtained by other methods, we need to extend it to the standard condition of 1 sun as τ depends on light intensity. For the S12 device, the highest intensity shown in Fig. 4(c) corresponds to $568\ \mu A$ of photocurrent or current density of 3.1 mA/cm^2. Under 1 sun illumination, our devices exhibit typical currents of 3.5-45.mA or 20-25 mA/cm^2. Assuming that the recombination rate continues to grow linearly with photocurrent, we can extrapolate Fig. 4c to 1 sun photocurrents and estimate that $\tau_{1\text{sun}} \approx 5\ \mu s$. This number has the same order of magnitude as the lifetime reported for a series

of $MAPb(I_{1-x}Br_x)_3$ perovskites, $\tau_{1sun} \approx 0.4 - 2$ μs [29] and is roughly consistent with the conclusion made in Ref. [30] that under ambient sunlight the electron-hole recombination is very slow, on the timescale of tens of microseconds.

In summary, noise spectroscopy has uncovered several relaxation processes in $MAPbI_3$ photovoltaic cells. We observe shot noise with near-unity Fano factor in devices with different thickness indicating that shot noise is dominated by single element of the cell, most probably the perovskite/spiro-OMeTAD interface. The1/f noise has contributions both from the light-absorbing perovskite layer and interfaces and its dependence on photocurrent indicates presence of defects induced by light and/or current. We also observe a GR contribution, corresponding to the bimolecular recombination in the bulk perovskite. The GR relaxation time agrees with the values reported in literature. Our analysis of the noise data relies on the spatial selectivity property of current noise spectroscopy, in which the most resistive elements in the device dominate the noise profile. This advantage should be useful for other devices with a complex stacked structure.

Acknowledgments

The work at University of Utah has been supported by NSF grants DMR1611421 and DMR1904221. The work at the National Renewable Energy Laboratory (NREL) was supported by De-risking Halide Perovskite Solar Cells program of the National Center for Photovoltaics, funded by Office of Energy Efficiency and Renewable Energy, Solar Energy Technologies Office, U.S. Department of Energy under Contract No. DE-AC36-08GO28308 with Alliance for Sustainable Energy, Limited Liability Company (LLC), the Manager and Operator of NREL. The views expressed in the article do not necessarily represent the views of the DOE or the U.S. Government. The U.S. Government retains and the publisher, by accepting the article for publication, acknowledges that the U.S. Government retains a nonexclusive, paid-up, irrevocable, worldwide license to publish or reproduce the published form of this work, or allow others to do so, for U.S. Government purposes.

Data Availability

The data that support the findings of this study are available from the corresponding author upon reasonable request.

Author Contributions

K.D., M.H, and L.D. performed the noise spectroscopy experiments; K.D. and A.R. designed the study and analyzed the data; F.Z. fabricated and provided the perovskite solar cell samples; K.D., A.R., and K.Z. wrote the manuscript. All authors collaborated on the data interpretation and have discussed the manuscript.

Competing Interests

The authors declare no competing interests.

References

[1] W. S. Yang, J. H. Noh, N. J. Jeon, Y. C. Kim, S. Ryu, J. Seo, and S. I. Seok. Science, **348**, 1234 (2015)
[2] M. A. Green, A. Ho-Bailliem, and H. J. Snaith. Nat. Photonics, **4**, 3623 (2014)
[3] S. D. Stranks and H. J. Snaith, Nat. Nanotechnol., **10**, 391 (2015)
[4] Best Research-Cell Efficiencies, NREL, https://www.nrel.gov/pv/assets/pdfs/best-research-cell-efficiencies.20190923.pdf (2019)
[5] Q. Dong, Y. Fang, Y. Shao, P. Mulligan, J. Qui, L. Cao, and J. Huang, Science, **347** 967 (2015).
[6] W. Yin, T. Shi, and Y. Yan, Appl. Phys. Lett. **104** 063903 (2014).
[7] S. D. Stranks, V. M. Burlakov, T. Leijtens, J. M. Ball, A. Goriely, and H. J. Snaith, Phys. Rev. Appl, **2**, 034007 (2014).
[8] Y. Li, H. Li, C. Zhong, G. Sini, and J. Brédas, NPJ Flexible Electronics, **1** 2 (2017).
[9] R. S. Sanchez and E. Mas-Marza, Solar Energy Materials & Solar Cells, **158**, 189 (2016).

[10] K. Mahmood, S. Sarwar, and M. T. Mehran, RSC Adv., **7**, 17044 (2017).
[11] E.G. Ioannidis, A. Tsormpatzoglou, D.H. Tassis, C A. Dimitriadis, F. Templier, and G. Kamarinos, J. Appl. Phys. 108, 106103 (2010).
[12] A. Carbone, C. Pennetta, and L. Reggiani, Appl. Phys. Lett., 95, 233303 (2009)
[13] A.A. Balandin, Nat. Nanotech., **8**, 549 (2013).
[14] G. Landi, C. Barone, C. Mauro, H.C. Neitzert, and S. Pagano, Scientific Reports, 6, 29685 (2016)
[15] J. Fan and J. Kakalios, Phys. Rev. B, **47**, 10903 (1993)
[16] V. K. Sangwan, M. Zhu, S. Clark, K. A. Luck, T. J. Marks, M. G. Kanatzidis, and M. C. Hersam, ACS Appl. Mater. Interfaces, **11** 14166 (2019).
[17] C. Barone, F. Lang, C. Mauro, G. Landi, J. Rappich, N. H. Nickel, B. Rech, S. Pagano & H. C. Neitzert, Scientific Reports, **6**, 34675 (2016).
[18] G. Ferrari and M. Sampietro, Rev. Sci. Instr. **73**, 7, 2717 (2002).
[19] T. K. Djidjou, Ying Chen, T. Basel, J. Shinar, and A. Rogachev, J. Appl. Phys. **117**, 11501 (2015).
[20] T. K. Djidjou, D. A. Bevans, S. Li, and A. Rogachev, IEEE Trans. on Electron Devices, **61**, 9, 3252 (2014).
[21] A. K. Jena, A. Kulkarni, and T. Miyasaka, Chem. Rev., **199**, 3036-3103 (2019)
[22] P. Lopez-Varo, J. A. Jiménez-Tejada, M. García-Rosell. S. Ravishankar, G. Garcia-Belmonte, J. Bisquert, and O. Almora, Adv. Energy Mater. **8** 1702772 (2018).
[23] F.E. Camino, V.V. Kuznetsov, E.E. Mendez, M.E. Gershenson, D. Reuter, P. Schafmeister, and A.D. Wieck, Phys. Rev. B, **68**, 073313 (2003).
[24] A. P. Dmitriev, M. E. Levinshtein, and S. L. Rumyantsev. J. Appl. Phys. 106, 024514 (2009).
[25] P. Dutta and P. M. Horn, Low-frequency fluctuations in solids: 1/f noise, Rev. Mod. Phys., **53**, 497 (1981).
[26] J.W. Lee, S.G. Kim, J.M. Yang, Y. Yang, N.G. Park, APL Mater. **7**, 041111 (2019)
[27] M. B. Johnston and L. Herz, Acc. Chem. Res., **49**, 146 (2016).
[28] J. Bisquert, *The Physics of Solar Cells: Perovskites, Organics, and Photovoltaic Fundamentals* (CRC Press, 2018).
[29] D. Kiermasch, P. Rieder, K. Tvingstedt, A. Baumann, and V. Dyakonov, Scientific Reports, 6, 39333 (2016).
[30] C.S. Ponesca, *et al*, J. Amer. Chem. Society, 136, 5189 (2014).